



<https://openaccess.leidenuniv.nl>

### **License: Article 25fa pilot End User Agreement**

This publication is distributed under the terms of Article 25fa of the Dutch Copyright Act (Auteurswet) with explicit consent by the author. Dutch law entitles the maker of a short scientific work funded either wholly or partially by Dutch public funds to make that work publicly available for no consideration following a reasonable period of time after the work was first published, provided that clear reference is made to the source of the first publication of the work.

This publication is distributed under The Association of Universities in the Netherlands (VSNU) 'Article 25fa implementation' pilot project. In this pilot research outputs of researchers employed by Dutch Universities that comply with the legal requirements of Article 25fa of the Dutch Copyright Act are distributed online and free of cost or other barriers in institutional repositories. Research outputs are distributed six months after their first online publication in the original published version and with proper attribution to the source of the original publication.

You are permitted to download and use the publication for personal purposes. All rights remain with the author(s) and/or copyrights owner(s) of this work. Any use of the publication other than authorised under this licence or copyright law is prohibited.

If you believe that digital publication of certain material infringes any of your rights or (privacy) interests, please let the Library know, stating your reasons. In case of a legitimate complaint, the Library will make the material inaccessible and/or remove it from the website. Please contact the Library through email: [OpenAccess@library.leidenuniv.nl](mailto:OpenAccess@library.leidenuniv.nl)

### **Article details**

Lin M-H., Potel C.M., Tehrani K.H.M.E., Heck A.J.R. Martin N.I. & Lemeer S. (2018), A new tool to reveal bacterial signaling mechanisms in antibiotic treatment and resistance, *Molecular and Cellular Proteomics* 17(12): 2496-2507.

Doi: 10.1074/mcp.RA118.000880

# A New Tool to Reveal Bacterial Signaling Mechanisms in Antibiotic Treatment and Resistance

## Authors

Miao-Hsia Lin, Clement M. Potel, Kamaledin H. M. E. Tehrani, Albert J. R. Heck, Nathaniel I. Martin, and Simone Lemeer

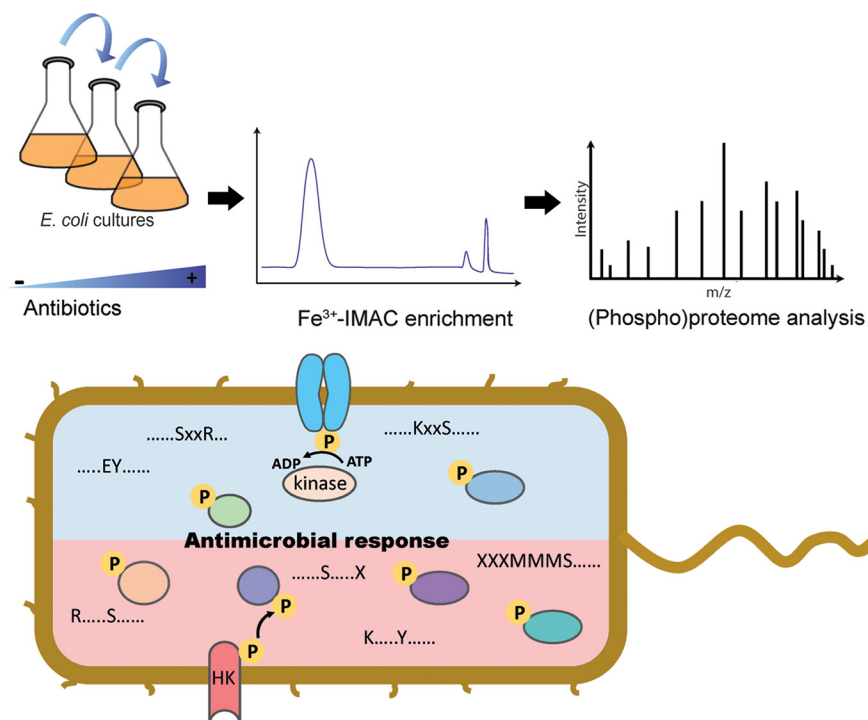
## Correspondence

s.m.lemeer@uu.nl

## In Brief

Changes in proteome and phosphoproteome have been determined in *E. coli* treated with the antibiotics colistin or ciprofloxacin and in a bona-fide *mcr-1* positive colistin resistant strain. The results reveal extensive phosphorylation on bacterial proteins and motif specific phosphorylation changes during resistance development. Moreover, regulated sites show high evolutionary conservation, indicating an important biological role. Together, this indicates that phosphorylation mediated signaling could be used as a specific target for drug design.

## Graphical Abstract



## Highlights

- Quantitative (phospho)proteome analysis of antibiotic treatment in *E. coli*.
- Largest bacterial phosphorylation catalogue.
- Specific phosphorylation motifs changes during resistance development.
- Phosphorylation mediated signaling could be a potential target for drug design.



# A New Tool to Reveal Bacterial Signaling Mechanisms in Antibiotic Treatment and Resistance\*<sup>§</sup>

Miao-Hsia Lin<sup>‡§</sup>, Clement M. Potel<sup>‡§</sup>, Kamaledin H. M. E. Tehrani<sup>¶</sup>,  
 Albert J. R. Heck<sup>‡§</sup>, Nathaniel I. Martin<sup>¶</sup>, and Simone Lemeer<sup>‡§</sup>||

**The rapid emergence of antimicrobial resistance is a major threat to human health. Antibiotics modulate a wide range of biological processes in bacteria and as such, the study of bacterial cellular signaling could aid the development of urgently needed new antibiotic agents. Due to the advances in bacterial phosphoproteomics, such a systemwide analysis of bacterial signaling in response to antibiotics has recently become feasible. Here we present a dynamic view of differential protein phosphorylation upon antibiotic treatment and antibiotic resistance. Most strikingly, differential phosphorylation was observed on highly conserved residues of resistance regulating transcription factors, implying a previously unanticipated role of phosphorylation mediated regulation. Using the comprehensive phosphoproteomics data presented here as a resource, future research can now focus on deciphering the precise signaling mechanisms contributing to resistance, eventually leading to alternative strategies to combat antimicrobial resistance. *Molecular & Cellular Proteomics* 17: 2496–2507, 2018. DOI: 10.1074/mcp.RA118.000880.**

Antimicrobial resistance (AMR)<sup>1</sup> has become one of the most serious threats to global health. At the rate at which resistance against antibiotics is currently rising, it is not inconceivable that we will be confronted with a situation in which the actual last resort antibiotics become ineffective. It is estimated that AMR could cause 10 million deaths every year by the year 2050 (1). In order to effectively combat the threat of AMR, understanding of the molecular mechanisms underlying resistance acquisition is essential.

The noun antibiotic, first described in 1941 by Selman Waksman, represents any small molecule made by a microbe that inhibits the growth of other microbes (2), but an alternative view of antibiotics envisions them as signaling molecules (3–5). The antibiotic colistin is a cationic cyclic decapeptide with a lipophilic fatty acyl side chain that is used as a last

resort antibiotic for the treatment of multidrug resistant Gram-negative infections (6). Alarming, a plasmid-mediated colistin resistance mechanism (*mcr-1* gene) has been reported in over 30 countries across five continents since it was first identified in 2015, raising major public health concern (7–9). Ciprofloxacin is another critically important antimicrobial with possible serious side effects (10) used to treat infections resistant to safer antibiotics. Ciprofloxacin is one of the most commonly prescribed fluoroquinolones in current medical practice, and its resistance rate has raised from 1.8% to 15.9% over only 10 years (11). Overall, the worldwide spread of AMR in recent years is a sobering reminder of our need to better understand resistance mechanisms in order to design new effective inhibitors.

While the characterization of resistance genes was already made possible by advances in functional metagenomic approaches, these methods cannot quantify proteins and decipher the potential bacterial signaling cascades involved in AMR. The study of bacterial cellular signaling in AMR and AMR acquisition could thus provide opportunities for the development of new therapeutic strategies. Bacteria are capable of modifying serine/threonine/tyrosine residues on proteins like eukaryotes, but in addition use two-component signaling that relies on histidine autophosphorylation of sensory kinases as the first component and aspartate phosphorylation of response regulators as the second component (12). Reversible protein phosphorylation is a well-established mechanism of regulating gene expression in response to a variety of environmental stress factors (13) and in recent years, growing evidence has linked two-component systems as well as serine/threonine/tyrosine kinase signaling to AMR (13–15). While mass-spectrometry-based proteomics has enabled the study of signaling dynamics on a global scale through the quantification of site-specific protein phosphorylation in eukaryotes, the study of bacterial phospho-signaling has largely lagged behind due to technical hurdles. Our recent

From the <sup>‡</sup>Biomolecular Mass Spectrometry and Proteomics, Bijvoet Center for Biomolecular Research, <sup>§</sup>Netherlands Proteomics Center, and <sup>¶</sup>Department of Chemical Biology & Drug Discovery, Utrecht Institute for Pharmaceutical Sciences, University of Utrecht, Utrecht, The Netherlands

Received May 29, 2018, and in revised form, September 12, 2018

Published, MCP Papers in Press, September 19, 2018, DOI 10.1074/mcp.RA118.000880

developments in this area enable us to reach in-depth coverage of bacterial phosphoproteomes (16, 17), offering the unprecedented opportunity to study signaling mechanisms during antibiotic treatment, resistance acquisition, and full resistance.

Here we set out to detect changes in proteome and phosphoproteome of antibiotic-treated bacteria in order to detect regulated expression and signaling that correlates with antibiotic susceptibility.

To this end we treated *Escherichia coli* with increasing doses of ciprofloxacin or colistin for several days, in order to decrease the susceptibility to the antibiotic. In the case of colistin, we also analyzed the (phospho)proteome of a *bona fide*, clinically isolated colistin resistant *E. coli* strain carrying the *mcr-1* plasmid. Our results indicate that antibiotic susceptibility rapidly increases for ciprofloxacin treatment, coinciding with extensive changes in phosphoproteome. For short-term colistin treatment, changes in phosphoproteome resemble the phosphoproteome of the *bona fide mcr-1* positive strain, despite the lack of a clear resistant phenotype, indicating that changes in signaling precede resistance development.

#### MATERIALS AND METHODS

**Bacterial Strains**—Two *E. coli* strains were used in this study: the wild-type *E. coli* strain W3110 (Coli Genetic Stock Center) and one clinically isolated *mcr-1* positive strain that carries the *mcr-1*-gene-containing plasmid, conferring colistin resistance as the minimal inhibitory concentration (MIC) was 8  $\mu\text{g/ml}$  (experimentally determined). This strain was isolated as part of routine diagnostic procedures in the University Medical Center Utrecht (Utrecht, the Netherlands) from a blood culture. This aspect of the study did not require consent or ethical approval by an institutional review board. The MIC of ciprofloxacin or colistin was determined by the dilution method in microtiter plates as previously described (18). For the *E. coli* W3110 wild-type strain, the MIC for colistin and ciprofloxacin was experimentally determined as 0.5  $\mu\text{g/ml}$  and 16  $\text{ng/ml}$ , respectively.

**Resistance Induction And Bacterial Cell Collections**—An overnight culture of wild-type *E. coli* strain was diluted 1:100 into Luria–Bertani medium with or without 4  $\text{ng/ml}$  ciprofloxacin, representing  $\frac{1}{4}$  the MIC of ciprofloxacin. After 24 h of incubation at 37 °C with shaking, the MIC was determined again. This same procedure was repeated until the MIC of ciprofloxacin increased to 128  $\text{ng/ml}$  (3 days) and 1,024  $\text{ng/ml}$  (7 days) which are 8- and 64-fold higher than the original MIC. The same approach was used for colistin in which the wild-type *E. coli* cells were culture with Luria–Bertani medium with  $\frac{1}{4}$  the MIC of colistin. However, no MIC increase was detected after 4 days up to 10 days of treatment. In order to detect the early response to colistin, phosphoproteome analysis was further performed on the 4-day treated *E. coli*. For all (phospho)proteomic analysis, 1 ml of culture was transferred to 100 ml culture medium including antibiotics. *E. coli* was subsequently grown to early-stationary phase ( $\text{OD}_{600} = 1.2$ ) after which samples for proteome and phosphoproteome analyses were collected. Briefly, bacterial cells were collected by centrifugation at 3,000  $g$  at 4 °C for 15 min. The cell pellets were washed twice with ice-cold PBS and stored at  $-80$  °C until further processes.

<sup>1</sup> The abbreviations used are: AMR, antimicrobial resistance; IMAC, immobilized metal ion affinity chromatography; *mcr-1*, mobilized colistin resistance gene; MIC, minimal inhibitory concentration; LC, liquid chromatography; GO, gene ontology.

**Cell Lysis And Protein Extraction**—All different *E. coli* cells with varied MICs to ciprofloxacin or colistin were lysed as described previously (16, 17). Briefly, cell pellets were resuspended with lysis buffer (100 mM Tris-HCl, pH 8.5, 7 M urea, 1% sodium deoxycholate (Sigma-Aldrich, Steinheim, Germany), 5 mM tris(2-carboxyethyl)phosphine, 30 mM 2-chloroacetamide, 10 U/ml DNase I, 1 mM magnesium chloride (Sigma Aldrich), 1% benzonase (Merck Millipore, Darmstadt, Germany), phosphoSTOP (Roche, Basel, Switzerland), and complete mini EDTA free (Roche)) and lysed by sonication for 45 min (20 s on, 40 s off) using a Bioruptor Plus. Cell debris was removed by ultracentrifugation (140,000  $g$  for 1 h at 4 °C). 1% benzonase was added to the supernatant, and the mixture was incubated at room temperature for 2 h. Protein concentration was determined by a Bradford protein assay (Bio-Rad, CA) using bovine serum albumin as the protein standard. Impurities were removed by methanol/chloroform protein precipitation as follows: 1 ml of supernatant was mixed with 4 ml of methanol (Sigma-Aldrich), 1 ml chloroform (Sigma-Aldrich) and 3 ml ultrapure water with thorough vortexing after each addition. The mixture was then centrifuged for 10 min at 5,000 rpm at room temperature. The upper layer was discarded, and 3 ml of methanol was added. After sonication and centrifugation (5,000 rpm, 10 min at room temperature), the solvent was removed and the precipitate was allowed to air dry. The pellet was resuspended in a buffer composed of 100 mM Tris-HCl, pH 8.5, 1% sodium deoxycholate, 5 mM tris(2-carboxyethyl)phosphine, and 30 mM 2-chloroacetamide. Trypsin (Sigma-Aldrich) and Lys-C (Wako, VA) proteases were respectively added to a 1:25 and 1:100 ratio (w/w), and protein digestion was performed overnight at room temperature.

**Peptide Desalting**—The tryptic peptide mixtures were acidified to pH 3.5 with 10% formic acid (Sigma-Aldrich) and centrifuged at 14,000 rpm for 10 min at 4 °C. The supernatant was then loaded on a 200 mg (3cc) tC18 Sep-Pak resin (Waters, MA), washed with  $2 \times 1$  ml of 0.1% formic acid, and peptides were eluted with 30% acetonitrile (Sigma). Eluted peptides were subsequently dried down using a lyophilizer and subjected to proteome analysis or phosphopeptide enrichment.

**Fe<sup>3+</sup>-IMAC Phosphopeptide Enrichment**—Enrichments were performed as previously described (17). Briefly, lyophilized peptides were dissolved in buffer containing 30% acetonitrile and 0.07% trifluoroacetic acid (TFA, Sigma-Aldrich), and the pH was adjusted to a value of 2.3 using 10% TFA prior to injection onto the Fe<sup>3+</sup>-IMAC column (Propac IMAC-10  $4 \times 50$  mm column, ThermoFisher Scientific). The elution buffer is composed of 0.3% NH<sub>4</sub>OH. UV-abs signal was recorded at the outlet of the column, at a wavelength of 280 nm. Collected phosphopeptides were immediately frozen in liquid nitrogen and subsequently dried down using a lyophilizer.

**LC-MS/MS**—Nanoflow LC-MS/MS analysis was performed by coupling an Agilent 1290 (Agilent Technologies, Middelburg, Netherlands) to an Orbitrap Q-Exactive HF (Thermo Scientific, Bremen, Germany). Lyophilized peptides were dissolved in loading buffer (10% formic acid (FA) in the case of proteome samples and 20 mM citric acid (Sigma-Aldrich) complemented with 1% formic acid in the case of phosphoproteome samples) and injected, trapped and washed on a pre-column (100  $\mu\text{m}$  inner diameter  $\times$  2 cm, packed with 3  $\mu\text{m}$  C18 resin, Reprosil PUR AQ, Dr. Maisch, Ammerbuch-Entringen, Germany, packed in-house) for 5 min at a flow rate of 5  $\mu\text{l/min}$  with 100% buffer A (0.1% FA, in HPLC-grade water). Peptides were then transferred to an analytical column (75  $\mu\text{m} \times 60$  cm Poroshell 120 EC-C18, 2.7  $\mu\text{m}$ , Agilent Technology, packed in-house) prior to separation at room temperature at a flow rate of 300 nL/min using a 115-min linear gradient, from 13% to 44% buffer B (0.1% FA, 80% acetonitrile (ACN)). Electrospray ionization was performed using 1.9-kV spray voltage and a capillary temperature of 320 °C. The mass spectrometer was operated in data-dependent acquisition mode: full scan MS

spectra ( $m/z$  375–1,600) were acquired in the Orbitrap at 60,000 resolution for a maximum injection time of 20 ms with an automatic gain control (AGC) target value of  $3e^6$ . Up to 12 precursors were selected for subsequent fragmentation and high-resolution higher energy collision-induced dissociation MS2 spectra were generated using a normalized collision energy of 27%. The intensity threshold to trigger MS2 spectra was set to  $2e^5$ , and the dynamic exclusion to 15 s. MS2 scans were acquired in the Orbitrap mass analyzer at a resolution of 30,000 (isolation window of 1.4 Th) with an AGC target value of  $1e^5$  charges and a maximum ion injection time of 50 ms. Precursor ions with unassigned charge state as well as charge state of 1+ or superior/equal to 6+ were excluded from fragmentation.

**Data Analysis**—MaxQuant software (version 1.6.0.1) was used to process the raw data files, which were searched against the database merging reviewed *E. coli* K12 sequences (*E. coli* K12 Uniprot database, March 2016, 4,434 entries) and *mcr-1* strain sequences (5,005 entries) and removing duplicates, with the following parameters: trypsin digestion (cleavage after lysine and arginine residues, even when followed by proline) with a maximum of three missed cleavages, fixed carbamidomethylation of cysteine residues, and variable modifications of methionine oxidation and protein N-terminal acetylation (19). In case of phosphoproteome analysis, the variable modification of phosphorylation on serine, threonine, tyrosine, histidine, and aspartate residues was also included. Mass tolerance was set to 4.5 ppm at the MS1 level and 20 ppm at the MS2 level. The false discovery rate was set to 1% at the peptide and protein level, an additional peptide score cutoff of 40 was used for modified peptides, and the minimum peptide length was set to seven residues. In terms of label-free quantification analysis, the match between runs function was used with the retention time window of 1 min. The MaxQuant output tables “evidence.txt” and “phospho (HDSTY)Sites.txt” from phosphoproteome dataset and “proteinGroups.txt” from proteome datasets were further used to calculate the identification number of unique phosphopeptides, phosphosites, and proteins. The table of phospho (HDSTY)Sites.txt and “proteinGroups.txt” were further used for quantification analysis at phosphoproteome and proteome level, respectively, using Perseus (version 1.6.0.2) (20). Known contaminants as provided by MaxQuant and identified in the samples were excluded from the analysis. The list of modified peptides was further filtered at the level of phospho-site localization using a localization probability threshold of 0.75 to derive all class I phospho-sites. To determine phosphorylation sites corresponding to dynamic profiles due to changes in phosphorylation state rather than protein abundance, we normalized the phosphosite level by the corresponding changes in protein abundance. To detect the complete matrix of intensities for on/off regulation in quantification analysis, missing value imputation was performed when all three values existed in at least on condition. The log2 scale of phosphosites or proteins intensity were subjected into a two-way analysis of variance test with a false discovery rate of less than 0.05.

**Bioinformatic Analysis**—The Gene Ontology (GO) analysis was performed with PANTHER (<http://www.pantherdb.org/>), with  $p$  value < 0.05. The KEGG pathway enrichment was performed using ClueGO app in Cytoscape (version 3.5.1) with the  $p$  value < 0.05 (21). Phosphorylation motifs were analyzed using the Motif- algorithm with occurrences set to 10 and significance set to 0.00001, using the whole genome sequence as background (22). Sequence logos were generated by iceLogo (23). For protein sequence alignment, full-length protein sequences were aligned using the Clustal X program with default settings and after alignment, phosphosite regions were displayed. All protein sequences from the same gene in different Gram-negative bacteria, relatively close to *E. coli*., were download from Uniprot.

**Experiment Design and Statistical Rationale**—Each sample was enriched in triplicate before being injected separately into the LC-MS/MS system. Each raw file was separately processed using the MaxQuant software. Triplicate analysis was sufficient to saturate the number of phosphosites detected.

## RESULTS

**Proteome Profiling Demonstrates Differential Protein Expression Triggered by Continuous Exposure to Antibiotics**—Wild-type *E. coli* cells were continuously exposed to low dosage, corresponding to one-quarter of the MIC, of either colistin or ciprofloxacin to decrease the antibiotic susceptibility and trigger AMR (Fig. 1A). For ciprofloxacin, we indeed observed a rapid increase in MIC, resulting in an eightfold higher MIC after 3 days and a 64-fold higher MIC after 7 days (Fig. 1A). For colistin, we did not observe a higher MIC after 4 days nor at 10 days of treatment, indicating a clear difference in response to the antibiotics used (Fig. 1A, [supplemental Fig. 1A](#)).

To comprehensively survey cellular signaling at early stages of antibiotic treatment and early resistance development, label-free quantification of both proteome and phosphoproteome was performed ([supplemental Fig. 1](#)). Due to the lack of a clear resistant phenotype at 10 days of colistin treatment, we focused our (phospho)proteome analysis to the 4-day time point in order to get insight into the early onset effects of colistin treatment. At a false discovery rate of 1% at the protein level, this resulted in the identification of 2,850 proteins ([supplemental Table 1](#)), from which 2,567 were quantified, achieving a similar coverage as previous *E. coli* proteome studies but within a significant shorter analysis time (24). Moreover, similar GO profiles were obtained at the proteome and genome levels, confirming the completeness of our proteome coverage ([supplemental Fig. 2](#)). We next evaluated these protein expression patterns to detect differential expression related to antibiotic treatment and resistance. Principle component analysis of colistin and ciprofloxacin proteome data clearly segregated samples into three groups. Furthermore, the analysis indicated that the serially passaged *E. coli* treated with a low dose of colistin are closer related to *mcr-1*-positive cells than to untreated cells, despite the lack of a clear resistant phenotype in serially passaged colistin treated *E. coli* (Fig. 1A and 1B). As expected, the phosphoethanolamine transferase coded by *mcr-1* was only identified in the *mcr-1* clinical strain (Fig. 1C). Surprisingly, several classes of proteins known to be involved in resistance exhibited significant changes in expression upon colistin treatment as well as in the *mcr-1* cells. The multidrug efflux pump (AcrA) as well as a variety of proteins involved in cell wall biogenesis, such as the Bam protein complex (25), LPS assembly outer membrane protein LptE (26), and the peptidoglycan biosynthesis proteins (MltA and MltB) (27) were more expressed in colistin serially passaged as well as in *mcr-1* cells (Fig. 1C and [supplemental Table 2](#)). Furthermore, the glycolysis/gluconeogenesis pathway and protein translation were down-regulated for both treated and resistant cells, which is consistent with the

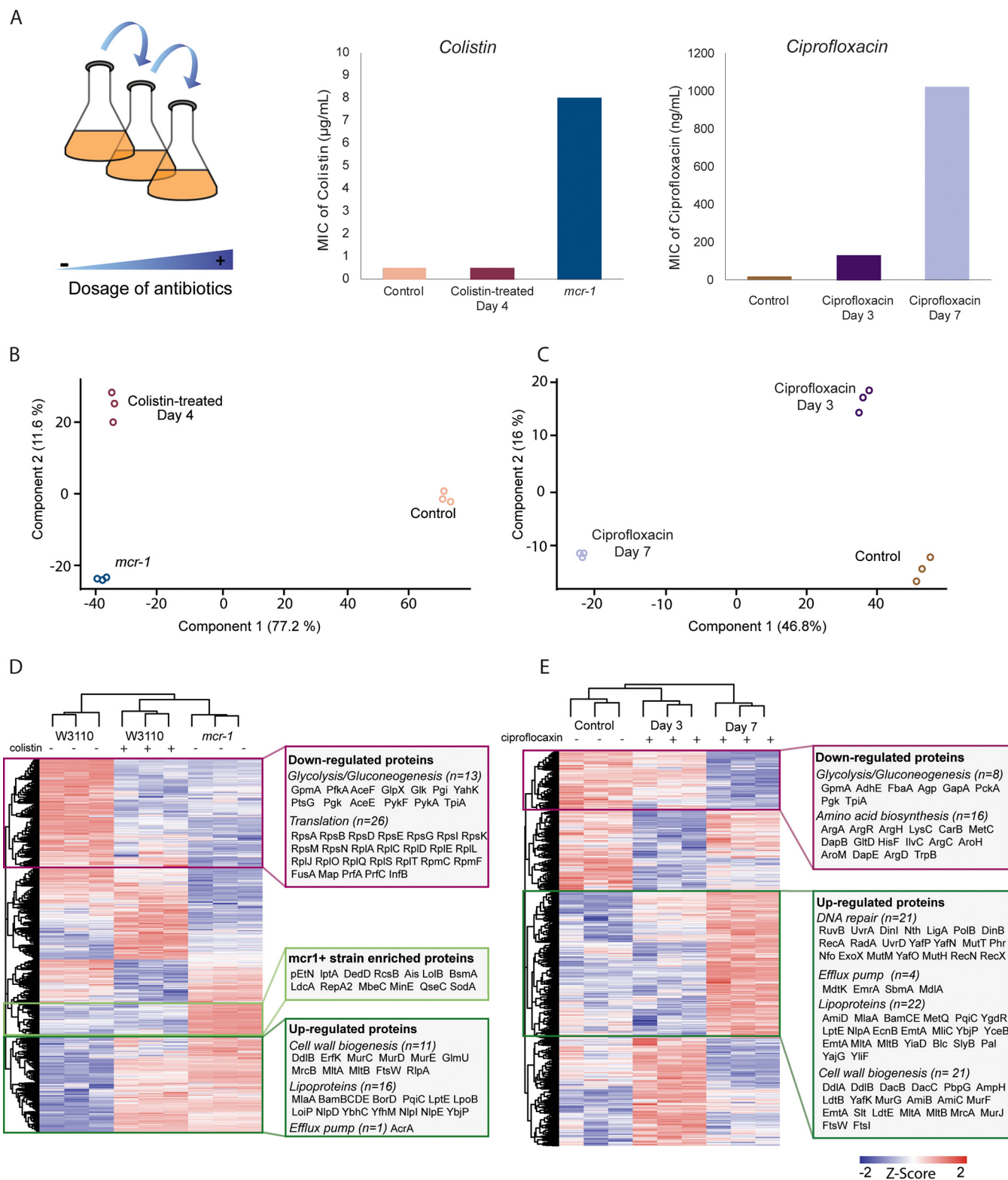


FIG. 1. Quantitative proteomic analysis of *E. coli* continuously exposed to colistin or ciprofloxacin. (A) Wild-type *E. coli* cells were continuously exposed to the antibiotics colistin or ciprofloxacin with the concentration being one quarter of the MIC. No MIC increase was noticed after 4 days of exposure to colistin, while the clinically isolated *mcr-1* strain exhibited a MIC of 8 µg/ml. However, after three and 7 days of exposure to ciprofloxacin, the MIC increased eightfold (128 ng/ml) and 64-fold (1,024 ng/ml), respectively. (B, C) Principle component analysis shows that the three replicates cluster together, indicating good reproducibility. (B) Pink circles represent the control wild-type *E. coli*

concept of compensatory fitness cost in developing resistance (28, 29) (Fig. 1C and supplemental Table 2).

For induced ciprofloxacin resistance, similar regulation patterns were observed, as expression levels of lipoproteins ( $n = 22$ ) or proteins involved in cell wall biogenesis ( $n = 21$ ) and cell cycle ( $n = 19$ ) were highly increased when antibiotic susceptibility decreased (Fig. 1D and supplemental Table 2). In agreement with ciprofloxacin targeting DNA gyrase activity, a significant number of DNA repair system proteins ( $n = 21$ ) were increasingly expressed when resistance developed (Fig. 1D and supplemental Table 2). Compared with colistin, ciprofloxacin induced the expression of a different panel of multidrug efflux system proteins, including MdtK, EmrA, SbmA, and MdlA proteins, which can be explained by the different nature of both antibiotics.

**Bacterial Protein Phosphorylation Is Far More Widespread Than Anticipated**—Bacteria, as well as other organisms, have developed several phosphorylation-dependent systems to adapt to environmental stresses, including the well-known two-component system, which constitutes one of the most sensitive and efficient regulatory mechanisms in bacteria. To get detailed insight into differential phosphorylation associated with antibiotic treatment, changes in antibiotic susceptibility, and resistance, we subsequently profiled the phosphoproteomes of all samples (supplemental Fig. 1). Our analysis resulted in the identification of 2,509 class I phosphosites (unambiguously localized) on 1,133 proteins (supplemental Table 3). In contrast to commonly used phosphoproteomics workflows, which are usually based on the combination of fractionation and phosphopeptide enrichment (30, 31), all experiments here were performed in triplicate, which was sufficient to saturate the number of sites (supplemental Fig. 3) with high quantification accuracy and reproducibility (Pearson correlation coefficient between 0.982 and 0.919, supplemental Fig. 4). In total, we quantified 3,872 phosphopeptides, which span around four orders magnitude of peptide ion signal, allowing us to look beyond classically observed phosphorylations on high abundant metabolic enzymes (Fig. 2A). In fact, phosphorylation events on several transcription factors and those indicating kinase activity were identified in the lowest-abundance range of the distribution. We therefore hypothesized that the dynamics of phosphorylation signaling networks induced by antibiotics could be well profiled (Fig. 2A). The comprehensive and parallel measurements of phosphoproteome and proteome allowed us, for the first time, to

investigate a possible correlation between a protein's abundance and its propensity to be phosphorylated. There is a weak but significant tendency between the number of identified phosphosites and increasing protein abundance (Fig. 2B, Pearson correlation as 0.65,  $p < 0.01$ ), which is similar to the profile in the human phosphoproteome (32). About 45% of identified proteins were phosphorylated on just one residue, whereas the remaining 55% were phosphorylated at multiple sites (Fig. 2C). In addition, the GO term enrichment of identified phosphorylated proteins correlates with the obtained proteome profile, suggesting that we achieved a comprehensive phosphoproteome coverage (supplemental Fig. 2). Moreover, the residue-specific phosphorylation pattern observed (Ser 56%, Thr 20%, Tyr 13%, Asp 5%, and His 5%; Fig. 2D) closely corresponds to previously published reports (33). When compared with the two existing databases, dbPSP and Uniprot, the work described here expands the known *E. coli* phosphoproteome by a factor of 4, and as a result, 89.6% of identified phosphosites ( $n = 2,248$ ) were observed for the first time (Fig. 2E) (34). Overall, this work indicates that bacterial phosphorylation is far more widespread than anticipated, as 40% of the identified proteins are phosphorylated.

**In-depth Quantitative Phosphoproteomics Enables Identification of Potential Regulators in Resistance Development**—Principal component analysis of the phosphoproteome data again segregated the *E. coli* cells according to antibiotic susceptibility (Fig. 3A and 3B). For ciprofloxacin, phosphoproteomes of 7-day-treated cells were more distinct from the 3-day-treated and nontreated cells. Surprisingly, for colistin, the 4-day-treated cells resembled the resistant *mcr-1* cells, again despite the presence of a clear resistant phenotype but in accordance with the proteome data. These results suggest that specific regulation at the phosphorylation level takes place upon antibiotics treatment, driving to a resistance-like phenotype (Fig. 3A). Indeed, a high percentage of identified phosphosites showed significant differential regulation during treatment and resistance: 460 phosphosites were significantly regulated in the colistin samples, while 911 were regulated upon ciprofloxacin treatment (analysis of variance test, false discovery rate  $< 0.05$ ; supplemental Table 4).

When looking closely at the significantly regulated phosphosites, we identified phosphorylation changes on several known resistance-related proteins. We observed increased phosphorylation of His717 on the ArcB sensor protein upon colistin treatment, a finding that is in agreement with previous

W3110 strain without colistin treatment. The purple circles represent the 4 days colistin treated *E. coli* cells, blue circles represent the *mcr-1* *E. coli* strain. This analysis of protein expression patterns clearly showed that colistin treated *E. coli* cells were closer to the *mcr-1* strain. (C) Purple and violet circles are representing *E. coli* cells harvested after 3 days or 7 days of ciprofloxacin treatment, respectively and brown circles represent the nontreated control. For ciprofloxacin, *E. coli* cells with an induced higher MIC (day 3, day 7) showed different patterns compared with nontreated *E. coli* cells. (D, E) Unsupervised clustering analysis of the changes in the proteome following induction of resistance to (D) colistin and (E) ciprofloxacin. The color code shows the relative abundance based on the Z-score. On the right, for each box that is highlighted in the cluster analysis, the enriched pathways are displayed. Proteins that belong to a specific cluster and participate in a certain pathway are indicated by their gene names. The pathway enrichment was performed using PANTHER ( $p$  values  $< 0.05$ ).

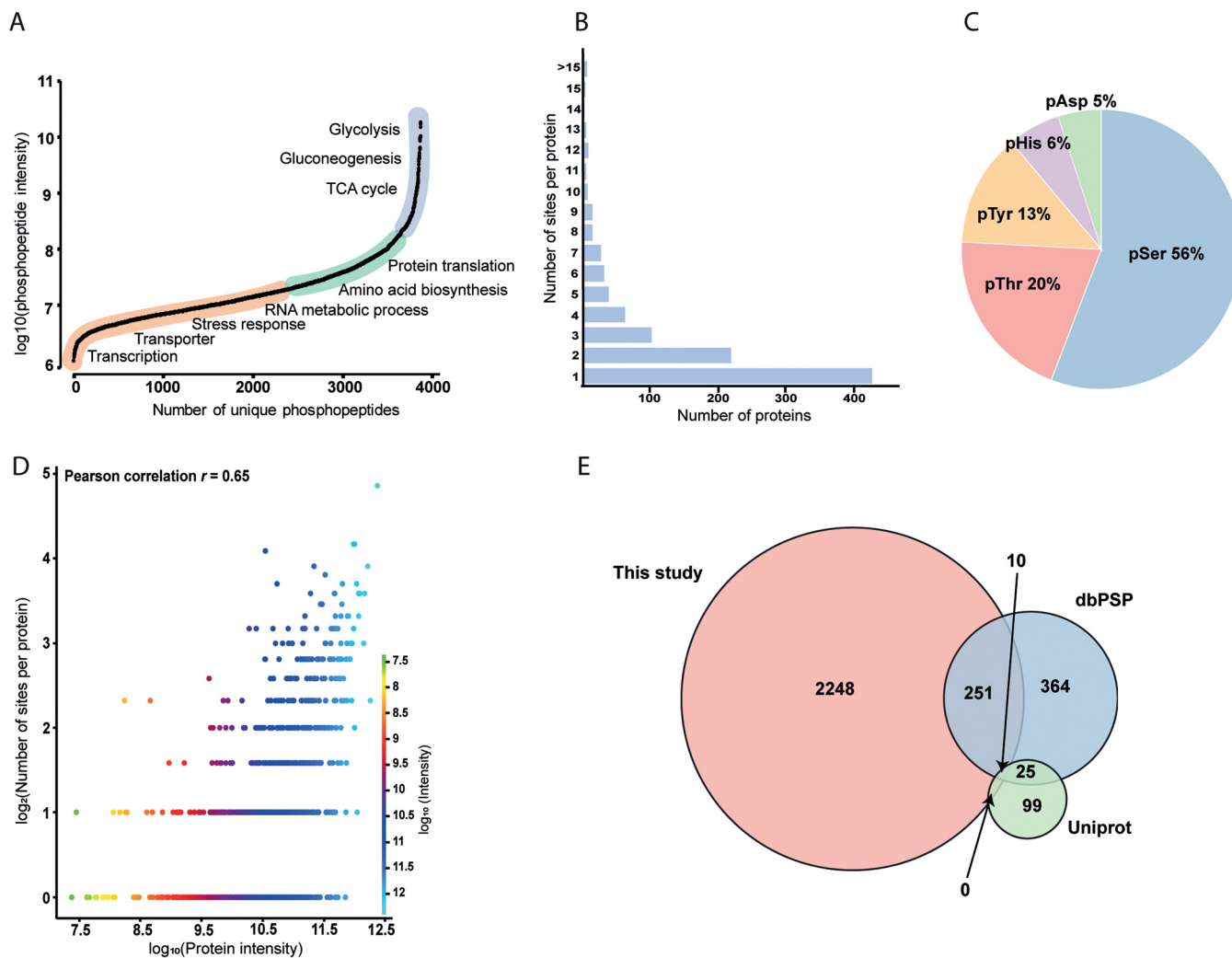


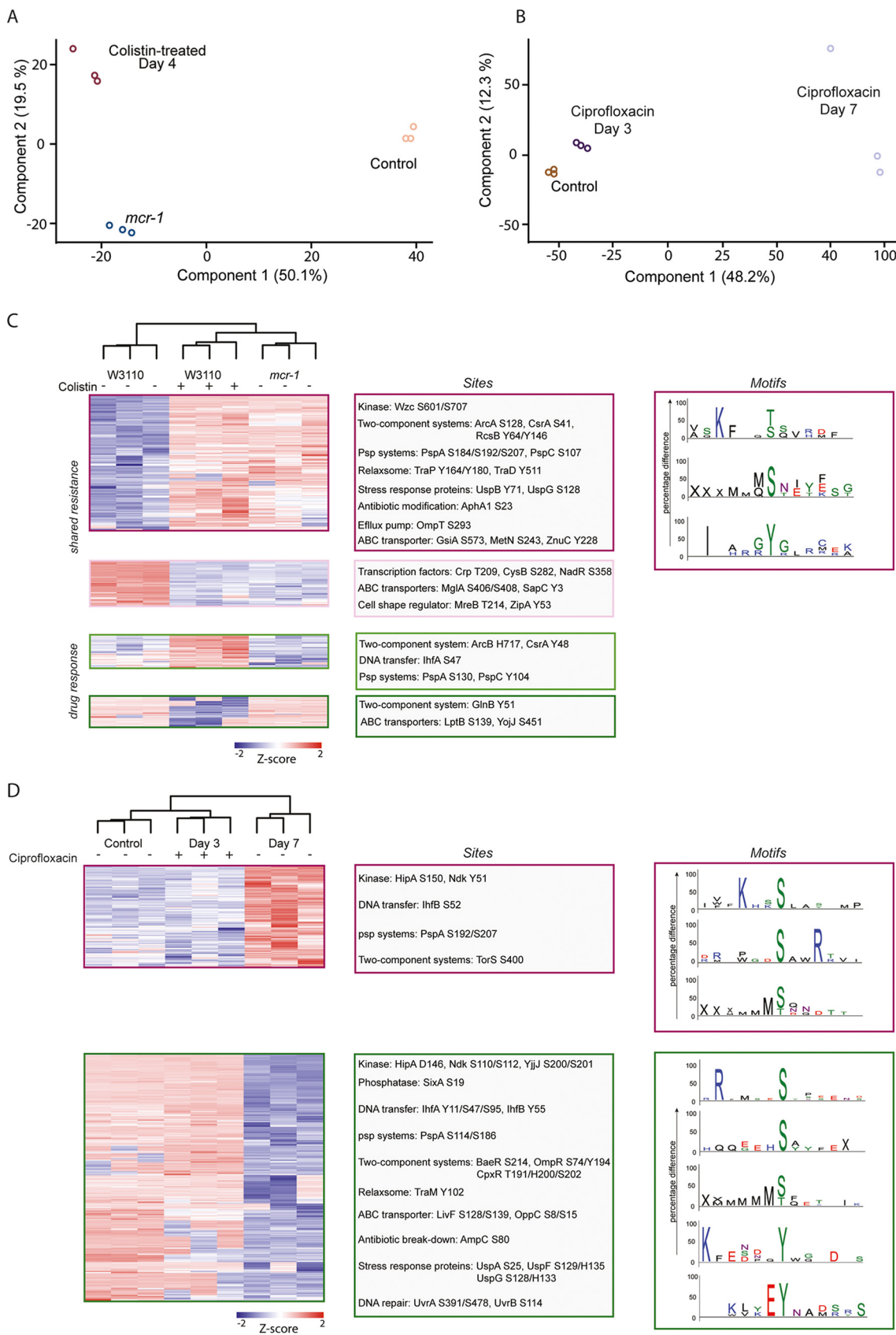
**FIG. 2. Comprehensive profiling of the *E. coli* phosphoproteome.** (A) Dynamic range of the quantifiable phosphopeptides with the corresponding overrepresented biological process GO terms. GO term enrichment was performed using PANTHER (<http://www.pantherdb.org/>) with  $p$  value  $< 0.05$ . (B) Correlation between the number of phosphosites per protein and protein abundance shows there is a weak correlation (Pearson correlation is 0.65). The color code indicates the protein abundance at log<sub>10</sub> scale. (C) Characterization of the phosphoproteins based on the number of phosphosites indicated that most of the proteins, around 45%, only have one phosphosite. (D) Phosphosite distribution across S/T/Y/H/D residues. (E) The overlap between phosphosites identified in this study and public databases, dbPSP and Uniprot, showing the up to 89.6% of phosphosites identified in this study are novel phosphosites.

studies showing that colistin stimulates the production of highly deleterious hydroxyl radicals, inducing high activity of the ArcAB two-component system as a resistance mechanism (35, 36). Phosphorylation levels of proteins involved in DNA transfer (relaxosome proteins: TraD, TraP) and integration host factor (IhfA) (37), universal stress proteins (UspB and UspG) (38), Psp system (PspA and PspC) (39), and drug efflux proteins (OmpT) (40) were also regulated in the colistin serially passaged *E. coli* (Fig. 3C and supplemental Table 4).

Similarly, differential phosphorylation of known resistance-related proteins was observed upon ciprofloxacin treatment (Fig. 3D and supplemental Table 4), for example on the DNA transfer-related proteins (TraM, IhfA, and IhfB), stress response proteins (UspA, UspF, and UspG) (38), psp system

(PspA) (39), and the antibiotics-degrading enzyme AmpC. Interestingly, phosphorylation of several DNA repair proteins (UvrA, UvrB, and UvrC) was significantly down-regulated in ciprofloxacin-resistant cells, implying that these phosphorylation events play a role in combating the effect of ciprofloxacin, which is a DNA gyrase inhibitor (Fig. 3D). ABC transporter and two-component system pathways, which are known to be related to evolution of resistance (14, 41), were significantly regulated in both colistin and ciprofloxacin treatments (Fig. 4). Though signal transduction via two-component systems is known to rely on reversible phosphorylation (12), regulated phosphosites identified here are mostly unknown, suggesting that the detailed signaling mechanisms underlying response and resistance to antibiotics are currently underestimated.





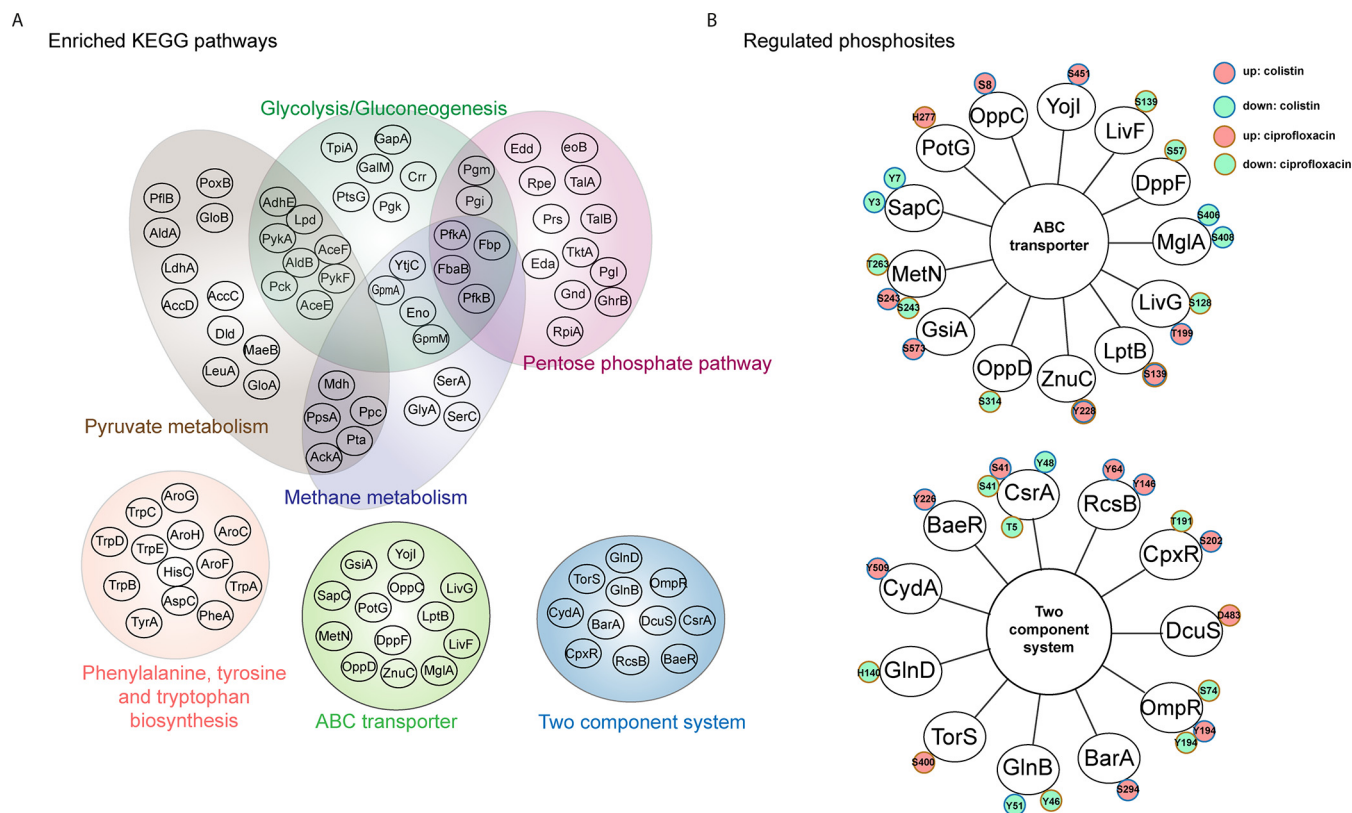


**FIG. 4. KEGG pathway enrichment analysis based on regulated phosphosites containing proteins from both colistin and ciprofloxacin treatments.** (A) In total, 555 phosphoproteins were subjected to KEGG pathway enrichment using Cytoscape with the ClueGO app. The pathways shown here are significantly enriched with  $p$  value  $< 0.05$ . Black circles represent the phosphoproteins containing regulated phosphosites, while the colored ellipses represent each overrepresented pathways. Proteins inside overlapping pathways indicate that these proteins are involved in multiple pathways. (B) The regulated phosphosites identified in ABC transporter and two component system upon colistin (blue circle) and ciprofloxacin (brown circle) treatments (green: down-regulated, pink: up-regulated).

Furthermore, we identify for the first time enriched phosphorylation motifs in different regulatory clusters, implying that specific kinase/phosphatase systems are involved in antibiotic response and resistance (Fig. 3C and 3D). As an example, we observed the motif KxxS, matching to the HipA kinase's substrate motif, on Ser239 of the GltX protein. Interestingly, the HipA kinase was phosphorylated at both Ser150 and Asp146, albeit respectively up- and down-regulated during antibiotic treatment, suggesting that those two phosphosites may play a role in the regulation of the kinase function

during resistance development (42). In addition, several specific tyrosine phosphorylation motifs were identified, suggesting the potential importance of tyrosine kinase-induced phosphorylation in resistance evolution (Fig. 3C and 3D). Protein phosphorylation occurring in the proximity of the protein N- or C terminus was highly enriched, consistent with findings in a previous study (33). We here demonstrate the possible importance of these terminal phosphorylation events in resistance development (Fig. 3C and 3D). As such terminal phosphorylation events are possibly bacteria specific, the kinases re-

**FIG. 3. Phosphoproteomes of *E. coli* changes extensively upon colistin and ciprofloxacin treatment.** As observed for the proteome analysis, triplicate phosphoproteomics samples clustered well together. (A) The pink circles represent the control *E. coli* W3110 strain without colistin treatment, whereas purple circles represent data from the serially passaged wild-type *E. coli* cells treated with colistin. Blue circles represent data from the *mcr-1* *E. coli* strain. Colistin-treated wild-type *E. coli* cells are in this analysis closer to the *mcr-1* strain, suggesting that common resistance mechanisms are partially shared. (B) For ciprofloxacin treatment, brown circles represent the control wild-type *E. coli* W3110 strain without ciprofloxacin treatment and purple and violet circles are representing the *E. coli* cells harvested after 3 days or 7 days treatment with ciprofloxacin, respectively. (C, D) Heatmap clustering of phosphorylation profiles after (C) colistin and (D) ciprofloxacin treatment. Each box represents a distinct unsupervised cluster profile across the different antibiotic susceptibilities. The color scale from blue to red indicates the Z-score, indicating decreased and increased phosphorylation. Regulated phosphosites in known resistance-related pathways are shown in the middle. Enriched phosphorylation motifs within particular clusters are displayed on the right, implicating that some specific kinases are involved in regulation. X was used to represent the N- or C-terminal position but not any particular amino acid. N-terminal phosphorylation was overrepresented in both treatments, while the C-terminal phosphorylation is only regulated in ciprofloxacin treatment. Three tyrosine phosphorylation motifs were enriched as well as four basophilic motifs.

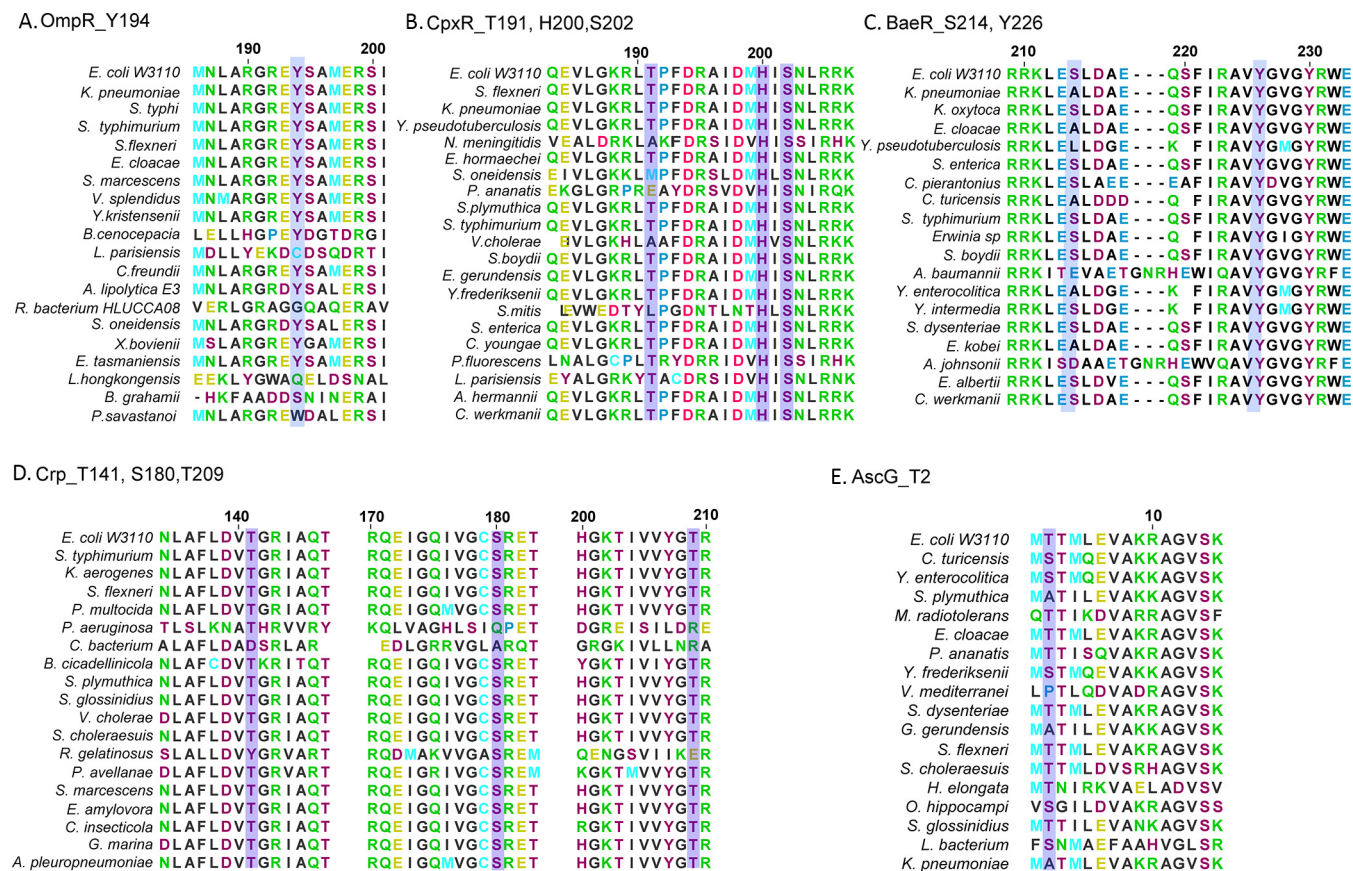


FIG. 5. Observed phosphosites are highly conserved on the helix-turn-helix regions of several transcription factors as revealed by sequence alignment across different bacteria. (A–C) Alignment of regulated phosphosites in the OmpR/PhoB subfamily transcription factors, including the Y194 on OmpR, H200 and S202 on CpxR, and S214 and Y226 on BaeR. (D, E) Alignment of phosphorylated residues on the non-OmpR/PhoB subfamily transcription factors, which are T141, S180, and T209 on Crp and T2 on AscG. These phosphosites have high conservation across different bacteria indicating a possible conserved role in regulations. Sequence alignment was performed with Clustal X with default parameters. The purple boxes represent the phosphosites identified in this study.

sponsible for these phosphorylations could represent adequate drug targets.

**Regulated Phosphosites Involved in DNA Transcription Display Evolutionary High Conservation Across Bacterial Species**—Phosphorylation on DNA transcriptional regulators is of particular interest because of its potential to influence bacterial cell growth and pathogenicity (13). This spurred us to assess the residue conservation among regulated phosphosites identified on known transcription factors, as a high level of conservation can indicate conserved biological function (13). Among identified regulated phosphosites, several residues on winged helix-turn-helix DNA-binding domains were highly conserved in proteobacteria. This includes residues on the C-terminal effector domain of the OmpR/PhoB subfamily transcription regulators such as Thr191, His200, and Ser202 residues on CpxR and Tyr194 on OmpR, and Ser214 and Tyr226 on BaeR (Fig. 5). Other evolutionary conserved phosphosites on helix-turn-helix domains were observed at Thr141, Ser180, and Thr209 of Crp as well as on Thr2 of the AscG transcription regulator (Fig. 5). Our data thus suggest that protein phosphorylation in the helix-turn-helix region

might be a widespread mechanism of transcriptional control of genes implicated in antibiotic resistance.

Phosphosites identified on transcription regulators such as Tyr64 and Tyr 146 on RcsB; Ser282 on CysB; Ser3 on SlyA; Thr62, Thr126, Ser129, and Ser135 on YebC; and His230 on YeiE were also found to be highly conserved among bacterial orthologues (supplemental Fig. 5). The observed up-regulation of the conserved transcriptional regulatory protein RcsB phosphosites, Tyr64 and Tyr146, for colistin serially passaged cells is consistent with previous reports establishing a link between the RcsCDB/F phospho-relay system and polymyxin resistance (43). In the same manner, high conservation of phosphorylated residues was found on other DNA-binding proteins, including Hns, StpA, HupA, and HupB, in which regulated phosphosites located both on DNA-binding or protein dimerization domains were found to be all highly conserved across bacteria (Fig. 6). Interestingly, the hns protein has been linked to multidrug resistance (44) and together with protein StpA coordinates OmpF porin gene expression and DNA conjugation in order to cope with environmental stress such as antibiotic administration (45, 46). In addition, histone-

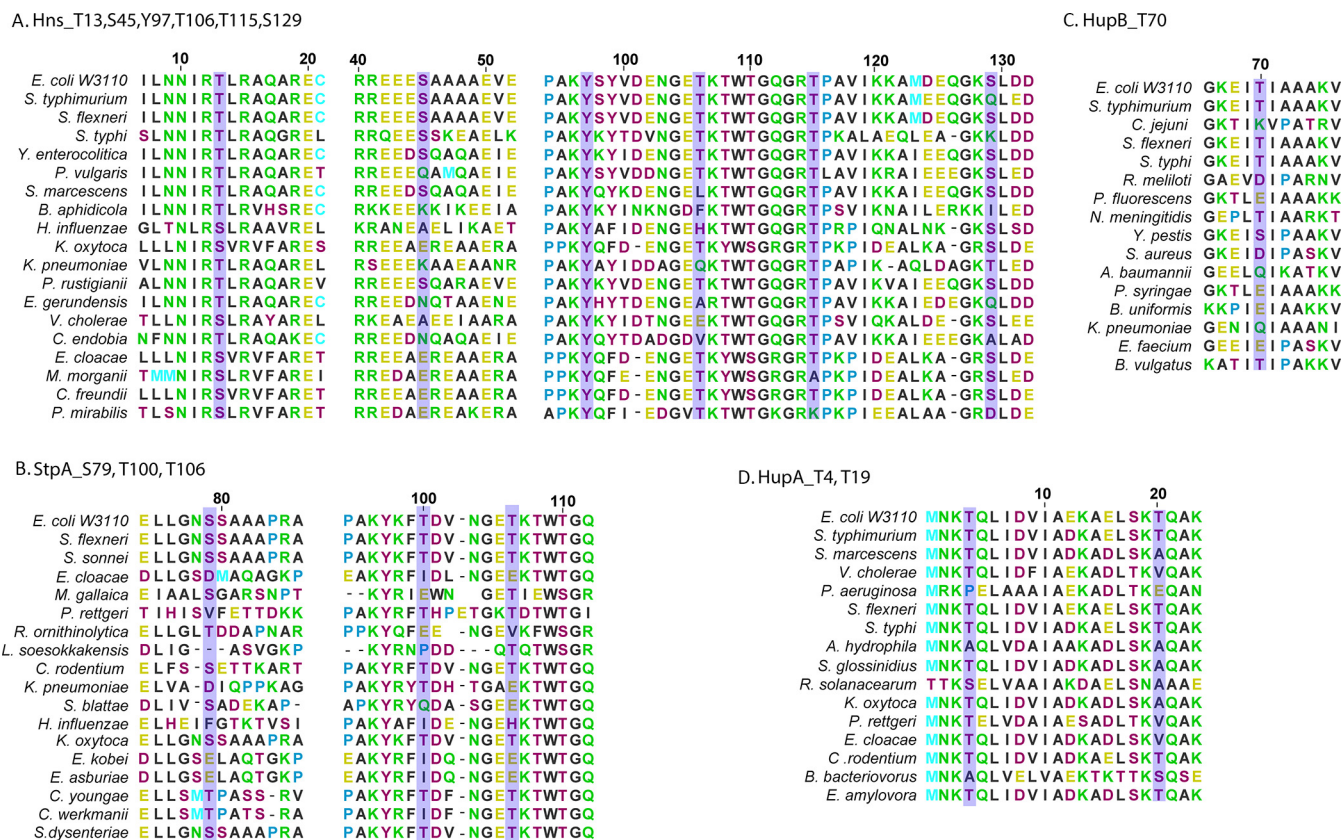


FIG. 6. Observed phosphosites are highly conserved in a variety of DNA-binding proteins across different bacteria. The phosphosites identified on DNA binding proteins (in purple boxes) include (A) T13, S45, Y97, T106, T115, and S129 on Hns, (B) S79, T100, and T106 on StpA, (C) T70 on HupB, and (D) T4 and T19 on HupA. Although S45 on Hns and T70 on HupB display slightly lower conservation, the high prevalence of acidic amino acids instead of Ser or Thr may reflect the fact that the negative charge is essential for protein functions.

like proteins HupA and HupB are the most common bacterial DNA-binding proteins responsible for nucleoid compaction; therefore, dynamic phosphorylation events located on DNA-binding region and the N-terminal tail might be similar to eukaryotic histones phosphorylations and serve as sensors of cellular stress, ultimately leading to resistance-related gene expression (47). Therefore, the well-known eukaryotic histone-code may have a prokaryotic counter-part.

DISCUSSION

The concept that regulated protein phosphorylation in its various facets could contribute to defining new drug targets is not new *per se*. However, the thorough investigation of phosphorylation signaling pathways in bacteria has been mostly neglected. Here we present the broadest bacterial phosphorylation catalogue, representing 2,509 phosphosites. Notably, the extent of phosphorylation regulation in bacteria is far more important than we anticipated, and the fact that only 10.4% of identified phosphosites ( $n = 261$ ) are reported in the public databases, Uniprot and dbPSP, make this study a valuable resource for future, indispensable work on deciphering signaling mechanisms involved in AMR.

We showed for the first time that specific phosphorylation motifs changed during resistance development. This is con-

sistent with the idea that bacterial Ser/Thr/Tyr kinases are involved in resistance development (48), which has been proposed but never comprehensively studied. Moreover, regulated phosphorylation sites located on transcription factors and other DNA-binding proteins showed high evolutionary conservation, indicating an important biological role. Finally, upon resistance development, we also observed specific regulation of N/C-terminal phosphorylation, which is unique to bacteria. Together, these regulated phosphorylation events during antibiotic treatment and resistance indicate that phosphorylation mediated signaling could be used as a specific target for drug design. In summary, we here describe the most comprehensive coverage of a bacterial phosphoproteome and monitor its dynamics upon perturbation by antibiotics. The unprecedented depth of our phospho-analysis, as well as the fact that significant reversible phosphorylation responses are observed upon antibiotic treatment opens up new avenues for research into novel alternative strategies to combat AMR. Future work should be aimed at understanding the contribution of each signaling pathway to resistance development.

*Acknowledgments*—We acknowledge Willem van Schaik and Axel Janssen in providing the *mcr-1+* strain and helpful discussions.

## DATA AVAILABILITY

All raw data that support the findings of this study have been deposited in jPOST repository (<https://repository.jpostdb.org>) with the accession number as JPST000388.

\* S.L. acknowledges support from the Netherlands Organization for Scientific Research through a VIDI grant (project 723.013.008). This work was supported by the Roadmap Initiative *Proteins@Work* funded by the Netherlands Organization for Scientific Research (project number 184.032.201), and the MSMed program, funded by the European Union's Horizon 2020 Framework Programme to A.J.R.H. (grant agreement number 686547). The authors declare no competing financial interest.

☐ This article contains supplemental material Tables 1–4 and Figs. 1–5.

|| To whom correspondence should be addressed: Biomolecular Mass Spectrometry and Proteomics Utrecht University Padualaan 8 3584 CA, Utrecht, the Netherlands. Tel.: +31-2539974. E-mail: s.m.lemeer@uu.nl.

Author contributions: M.-H.L., C.M.P., K.H.T., N.I.M., and S.L. designed research; M.-H.L., C.M.P., K.H.T., and S.L. performed research; M.-H.L., C.M.P., and S.L. contributed new reagents/analytical tools; M.-H.L. and C.M.P. analyzed data; and M.-H.L., C.M.P., A.J.R.H., and S.L. wrote the paper.

## REFERENCES

- O'Neill, J. (2016) Tackling drug-resistant infections globally: Final report and recommendations [https://amr-review.org/sites/default/files/160525\\_Final%20paper\\_with%20cover.pdf](https://amr-review.org/sites/default/files/160525_Final%20paper_with%20cover.pdf)
- Clardy, J., Fischbach, M. A., and Currie, C. R. (2009) The natural history of antibiotics. *Curr. Biol.* **19**, R437–R441
- Goh, E. B., Yim, G., Tsui, W., McClure, J., Surette, M. G., and Davies, J. (2002) Transcriptional modulation of bacterial gene expression by sub-inhibitory concentrations of antibiotics. *Proc. Natl. Acad. Sci. U.S.A.* **99**, 17025–17030
- Hoffman, L. R., D'Argenio, D. A., MacCoss, M. J., Zhang, Z., Jones, R. A., and Miller, S. I. (2005) Aminoglycoside antibiotics induce bacterial biofilm formation. *Nature* **436**, 1171–1175
- Yim, G., Wang, H. H., and Davies, J. (2007) Antibiotics as signalling molecules. *Phil. Trans. Royal Society London Series B* **362**, 1195–1200
- Falagas, M. E., and Kasiakou, S. K. (2005) Colistin: the revival of polymyxins for the management of multidrug-resistant gram-negative bacterial infections. *Clin. Infect. Disease* **40**, 1333–1341
- Liu, Y. Y., Wang, Y., Walsh, T. R., Yi, L. X., Zhang, R., Spencer, J., Doi, Y., Tian, G., Dong, B., Huang, X., Yu, L. F., Gu, D., Ren, H., Chen, X., Lv, L., He, D., Zhou, H., Liang, Z., Liu, J. H., and Shen, J. (2016) Emergence of plasmid-mediated colistin resistance mechanism MCR-1 in animals and human beings in China: A microbiological and molecular biological study. *Lancet. Infect. Diseases* **16**, 161–168
- Wang, Y., Tian, G. B., Zhang, R., Shen, Y., Tyrrell, J. M., Huang, X., Zhou, H., Lei, L., Li, H. Y., Doi, Y., Fang, Y., Ren, H., Zhong, L. L., Shen, Z., Zeng, K. J., Wang, S., Liu, J. H., Wu, C., Walsh, T. R., and Shen, J. (2017) Prevalence, risk factors, outcomes, and molecular epidemiology of mcr-1-positive *Enterobacteriaceae* in patients and healthy adults from China: An epidemiological and clinical study. *Lancet. Infect. Diseases* **17**, 390–399
- Wang, R., van Dorp, L., Shaw, L. P., Bradley, P., Wang, Q., Wang, X., Jin, L., Zhang, Q., Liu, Y., Rieux, A., Dorai-Schneiders, T., Weinert, L. A., Iqbal, Z., Didelot, X., Wang, H., and Balloux, F. (2018) The global distribution and spread of the mobilized colistin resistance gene mcr-1. *Nature Commun.* **9**, 1179
- Fasugba, O., Gardner, A., Mitchell, B. G., and Mnataganian, G. (2015) Ciprofloxacin resistance in community- and hospital-acquired *Escherichia coli* urinary tract infections: A systematic review and meta-analysis of observational studies. *BMC Infect. Diseases* **15**, 545
- Blaettler, L., Mertz, D., Frei, R., Elzi, L., Widmer, A. F., Battegay, M., and Flückiger, U. (2009) Secular trend and risk factors for antimicrobial resistance in *Escherichia coli* isolates in Switzerland 1997–2007. *Infection* **37**, 534–539
- Kobir, A., Shi, L., Boskovic, A., Grangeasse, C., Franjevic, D., and Mijakovic, I. (2011) Protein phosphorylation in bacterial signal transduction. *Biochim. Biophys. Acta* **1810**, 989–994
- Kalantari, A., Derouiche, A., Shi, L., and Mijakovic, I. (2015) Serine/threonine/tyrosine phosphorylation regulates DNA binding of bacterial transcriptional regulators. *Microbiology* **161**, 1720–1729
- Tiwari, S., Jamal, S. B., Hassan, S. S., Carvalho, P. V. S. D., Almeida, S., Barh, D., Ghosh, P., Silva, A., Castro, T. L. P., and Azevedo, V. (2017) Two-component signal transduction systems of pathogenic bacteria as targets for antimicrobial therapy: An overview. *Frontiers Microbiol.* **8**, 1878
- Pensinger, D. A., Schaezner, A. J., and Sauer, J. D. (2018) Do shoot the messenger: PASTA kinases as virulence determinants and antibiotic targets. *Trends Microbiol.* **26**, 56–69
- Potel, C. M., Lin, M. H., Heck, A. J. R., and Lemeer, S. (2018) Widespread bacterial protein histidine phosphorylation revealed by mass spectrometry-based proteomics. *Nat. Methods* **15**, 187–190
- Potel, C. M., Lin, M. H., Heck, A. J. R., and Lemeer, S. (2018) Defeating major contaminants in Fe(3+)-immobilized metal ion affinity chromatography (IMAC) phosphopeptide enrichment. *Mol. Cell. Proteomics* **17**, 1028–1034
- Hengzhuang, W., Wu, H., Ciofu, O., Song, Z., and Høiby, N. (2011) Pharmacokinetics/pharmacodynamics of colistin and imipenem on mucoid and nonmucoid *Pseudomonas aeruginosa* biofilms. *Antimicrob. Agents Chemother.* **55**, 4469–4474
- Cox, J., and Mann, M. (2008) MaxQuant enables high peptide identification rates, individualized p.p.b.-range mass accuracies and proteome-wide protein quantification. *Nature Biotechnol.* **26**, 1367–1372
- Tyanova, S., Temu, T., Sinitcyn, P., Carlson, A., Hein, M. Y., Geiger, T., Mann, M., and Cox, J. (2016) The Perseus computational platform for comprehensive analysis of (prote)omics data. *Nat. Methods* **13**, 731–740
- Bindea, G., Mlecnik, B., Hackl, H., Charoentong, P., Tosolini, M., Kirilovsky, A., Fridman, W. H., Pagès, F., Trajanoski, Z., and Galon, J. (2009) ClueGO: A Cytoscape plug-in to decipher functionally grouped gene ontology and pathway annotation networks. *Bioinformatics* **25**, 1091–1093
- Schwartz, D., and Gygi, S. P. (2005) An iterative statistical approach to the identification of protein phosphorylation motifs from large-scale data sets. *Nature Biotechnol.* **23**, 1391–1398
- Colaert, N., Helsens, K., Martens, L., Vandekerckhove, J., and Gevaert, K. (2009) Improved visualization of protein consensus sequences by ice-Logo. *Nat. Methods* **6**, 786–787
- Soufi, B., Krug, K., Harst, A., and Macek, B. (2015) Characterization of the *E. coli* proteome and its modifications during growth and ethanol stress. *Frontiers Microbiol.* **6**, 103
- Knowles, T. J., Scott-Tucker, A., Overduin, M., and Henderson, I. R. (2009) Membrane protein architects: The role of the BAM complex in outer membrane protein assembly. *Nat. Rev. Microbiol.* **7**, 206–214
- Gu, Y., Stansfeld, P. J., Zeng, Y., Dong, H., Wang, W., and Dong, C. (2015) Lipopolysaccharide is inserted into the outer membrane through an intramembrane hole, a lumen gate, and the lateral opening of LptD. *Structure* **23**, 496–504
- Cavallari, J. F., Lamers, R. P., Scheurwater, E. M., Matos, A. L., and Burrows, L. L. (2013) Changes to its peptidoglycan-remodeling enzyme repertoire modulate beta-lactam resistance in *Pseudomonas aeruginosa*. *Antimicrob. Agents Chemother.* **57**, 3078–3084
- Händel, N., Schuurmans, J. M., Brul, S., and ter Kuile, B. H. (2013) Compensation of the metabolic costs of antibiotic resistance by physiological adaptation in *Escherichia coli*. *Antimicrob. Agents Chemother.* **57**, 3752–3762
- Zampieri, M., Enke, T., Chubukov, V., Ricci, V., Piddock, L., and Sauer, U. (2017) Metabolic constraints on the evolution of antibiotic resistance. *Mol. Syst. Biol.* **13**, 917
- Mijakovic, I., and Macek, B. (2012) Impact of phosphoproteomics on studies of bacterial physiology. *FEMS Microbiol. Rev.* **36**, 877–892
- Soares, N. C., Spät, P., Krug, K., and Macek, B. (2013) Global dynamics of the *Escherichia coli* proteome and phosphoproteome during growth in minimal medium. *J. Proteome Res.* **12**, 2611–2621

32. Sharma, K., D'Souza, R. C., Tyanova, S., Schaab, C., Wiśniewski, J. R., Cox, J., and Mann, M. (2014) Ultradeep human phosphoproteome reveals a distinct regulatory nature of Tyr and Ser/Thr-based signaling. *Cell Reports* **8**, 1583–1594
33. Lin, M. H., Sugiyama, N., and Ishihama, Y. (2015) Systematic profiling of the bacterial phosphoproteome reveals bacterium-specific features of phosphorylation. *Sci. Signal* **8**, rs10
34. Pan, Z., Wang, B., Zhang, Y., Wang, Y., Ullah, S., Jian, R., Liu, Z., and Xue, Y. (2015) dbPSP: A curated database for protein phosphorylation sites in prokaryotes. *Database (Oxford)* **2015**, bav031
35. Loui, C., Chang, A. C., and Lu, S. (2009) Role of the ArcAB two-component system in the resistance of *Escherichia coli* to reactive oxygen stress. *BMC Microbiol.* **9**, 183
36. Yu, Z., Zhu, Y., Qin, W., Yin, J., and Qiu, J. (2017) Oxidative stress induced by polymyxin E is involved in rapid killing of *Paenibacillus polymyxa*. *BioMed Res. Int.* **2017**, 5437139
37. Frost, L. S., and Koraimann, G. (2010) Regulation of bacterial conjugation: Balancing opportunity with adversity. *Future Microbiol.* **5**, 1057–1071
38. Nachin, L., Nannmark, U., and Nyström, T. (2005) Differential roles of the universal stress proteins of *Escherichia coli* in oxidative stress resistance, adhesion, and motility. *J. Bacteriol.* **187**, 6265–6272
39. Vega, N. M., Allison, K. R., Khalil, A. S., and Collins, J. J. (2012) Signaling-mediated bacterial persister formation. *Nature Chem. Biol.* **8**, 431–433
40. Li, H., Wang, B. C., Xu, W. J., Lin, X. M., and Peng, X. X. (2008) Identification and network of outer membrane proteins regulating streptomycin resistance in *Escherichia coli*. *J. Proteome Res.* **7**, 4040–4049
41. Moussatova, A., Kandt, C., O'Mara, M. L., and Tieleman, D. P. (2008) ATP-binding cassette transporters in *Escherichia coli*. *Biochim. Biophys. Acta* **1778**, 1757–1771
42. Correia, F. F., D'Onofrio, A., Rejtar, T., Li, L., Karger, B. L., Makarova, K., Koonin, E. V., and Lewis, K. (2006) Kinase activity of overexpressed HipA is required for growth arrest and multidrug tolerance in *Escherichia coli*. *J. Bacteriol.* **188**, 8360–8367
43. Erickson, K. D., and Detweiler, C. S. (2006) The Rcs phosphorelay system is specific to enteric pathogens/commensals and activates ydel, a gene important for persistent *Salmonella* infection of mice. *Mol. Microbiol.* **62**, 883–894
44. Nishino, K., and Yamaguchi, A. (2004) Role of histone-like protein H-NS in multidrug resistance of *Escherichia coli*. *J. Bacteriol.* **186**, 1423–1429
45. Shiraishi, K., Ogata, Y., Hanada, K., Kano, Y., and Ikeda, H. (2007) Roles of the DNA binding proteins H-NS and StpA in homologous recombination and repair of bleomycin-induced damage in *Escherichia coli*. *Genes Genet. Sys.* **82**, 433–439
46. Deighan, P., Free, A., and Dorman, C. J. (2000) A role for the *Escherichia coli* H-NS-like protein StpA in OmpF porin expression through modulation of micF RNA stability. *Mol. Microbiol.* **38**, 126–139
47. Sawicka, A., and Seiser, C. (2014) Sensing core histone phosphorylation—A matter of perfect timing. *Biochim. Biophys. Acta* **1839**, 711–718
48. Wright, D. P., and Uljasz, A. T. (2014) Regulation of transcription by eukaryotic-like serine-threonine kinases and phosphatases in Gram-positive bacterial pathogens. *Virulence* **5**, 863–885